Structural features of lipid A of *Rickettsia typhi*

M. FODOROVÁ, P. VADOVIČ, R. TOMAN[*]

Department of Rickettsiology, Laboratory for Diagnosis and Prevention of Rickettsial and Chlamydial Infections, Institute of Virology, Slovak Academy of Sciences, Dúbravská cesta 9, 845 05 Bratislava, Slovak Republic

Summary. – Lipid A isolated from the *Rickettsia typhi* lipopolysaccharide (LPS) was investigated for its composition and structure using chemical analyses, gas chromatography-mass spectrometry (GC-MS), and electrospray ionization (ESI) combined with the tandem mass spectrometry (MS/MS). Our studies revealed a noticeable compositional and structural heterogeneity of lipid A with respect to the content of phosphate groups and the degree of acylation. It appeared that at least two molecular species were present in lipid A. The major species represented the hexaacyl lipid A consisting of the β-(1→6)-linked D-glucosamine (GlcN) disaccharide backbone carrying two phosphate groups. One of them was linked to the glycosidic hydroxyl group of the reducing GlcN I and the other was ester linked to the O-4´ position of the non-reducing GlcN II. The primary fatty acids consisted of two 3-hydroxytetradecanoic [C14:0(3-OH)] and two 3-hydroxyhexadecanoic [C16:0(3-OH)] acids. The former were ester- and the latter amide-linked to both GlcN. Two secondary fatty acids were represented by the octadecanoic (C18:0) and hexadecanoic (C16:0) acids that were ester-linked at the N-2´ and O-3´ positions, respectively. In the minor lipid A species, ester-linked C18:0 was substituted by C16:0 at the C16:0(3-OH) of GlcN II. The *R. typhi* lipid A resembles structurally the classical forms of enterobacterial lipids A with high endotoxicity.

Keywords: Rickettsia typhi; lipopolysaccharide; lipid A; chemical composition; structure

Introduction

Rickettsia typhi, the etiological agent of endemic (murine) typhus, is a small obligate intracellular parasite requiring the host eukaryotic cells for replication. It is a Gram-negative bacterium maintained in rodents and transmitted to humans by the rat flea *Xenopsylla cheopis*. Humans are infected by a contamination of disrupted skin or respiratory tract with infected flea feces (Azad *et al.*, 1997). Endemic typhus is

a relatively mild, acute febrile illness characterized mainly by headache, fever, and macular rash (Snyder, 1965; Raoult and Roux, 1997). The disease can be diagnosed using serological, clinical, and epidemiological testing (Whiteford *et al.*, 2001). Serological diagnosis of murine typhus is quite often ambiguous due to the absence of specific and highly sensitive antigens. *R. typhi* shares (OX) antigens of *Proteus vulgaris* and the antibodies produced against it cross-react with the strains of *P. vulgaris* (Shirai *et al.*, 1975). The bacterium possesses at least two different types of antigens. One of them is a group-specific antigen and the other is a species-specific antigen. It has been assumed that LPS belongs to the group-specific antigens of *R. typhi* (Amano *et al.*, 1998).

It has been known for a long time that the *R. typhi* LPS is responsible for several endotoxic activities such as lethal toxicity, pyrogenicity, and Schwartzman reaction (Schramek *et al.*, 1977; Fumarola *et al.*, 1979), but the structure/function relationship studies have not been performed yet. It was postulated in the past that lipid A constitutes the endotoxically active region of the LPS molecule, expressing all the patho-

[*]Corresponding author. E-mail: virutoma@savba.sk; fax: +4212-54774284.
Abbreviations: ESI = electrospray ionization; GC = gas chromatography; GlcN = glucosamine; C16:0 = hexadecanoic acid; C16:0(3-OH) = 3-hydroxyhexadecanoic acid; C14:0(3-OH) = 3-hydroxytetradecanoic acid; LPS = lipopolysaccharide; MS = mass spectrometry; *m/z* = mass-to-charge ratio; C18:0 = octadecanoic acid; QuiN = quinovosamine; MS/MS = tandem mass spectrometry; C14:1n3 = 3-tetradecenoic acid; TLC = thin layer chromatography

physiological effects known to be induced by the complete LPS molecule (Zähringer *et al.*, 1994). Thus, knowledge of the lipid A structure is a prerequisite for understanding of the molecular mechanisms operating during endotoxemia (Zähringer *et al.*, 1999). To our best knowledge, there has been no work published dealing with the structure of lipid A of *R. typhi* thus far. In this paper, we report for the first time its structural features based mainly on the results of GC-MS and ESI-MS/MS analyses.

Materials and Methods

Cultivation and purification of the R. typhi cells. R. typhi was obtained from the strain collection of the Laboratory for Diagnosis and Prevention of Rickettsial and Chlamydial Infections, Institute of Virology, Slovak Academy of Sciences, Bratislava, Slovak Republic. The cells were propagated in embryonated, antibiotic-free, and pathogen-free eggs. All laboratory procedures involving the handling of live bacteria were carried out at Biosafety Level 3. The propagated bacteria were inactivated with 0.5% phenol and purified by rate-zonal sedimentation in gradients of Renografin (Ultravist 370, 0.769 g/ml iopromide, Schering). Gradients were centrifuged at 112,500 x g for 90 mins at 4°C. The fractions containing the *R. typhi* cells were collected and the Renografin was removed by sedimentation. The bacterial pellet was resuspended in PBS and stored at -80°C.

Isolation of LPS and lipid A of R. typhi. The purified cells (1 g) were suspended in 50 mmol/l Tris-HCl buffer (100 ml, pH 7.5) and treated simultaneuosly with RNase and DNase I, both from bovine pancreas (Boehringer) at 37°C for 16 hrs. The cells were then treated with trypsin (Serva) at 37°C for 90 mins followed by proteinase K from *Tritirachium album* (Sigma) at 37°C for 16 hrs. After enzyme treatment, the cell suspension was centrifuged at 14,000 x g, 10°C for 50 mins and the sediment was washed with acetone. The dried cells were extracted with chloroform-methanol (2:1, v/v) at 20°C overnight to remove phospholipids. The extraction was repeated with the fresh solvent mixture for 2 hrs. The cell suspension was centrifuged at 3,000 x g for 20 mins and the sediment was suspended in preheated deionized water (100 ml, 68°C) and extracted with an equal volume of aqueous 90% phenol as described (Škultéty *et al.,* 1998). The yield of LPS was 20.1 mg (2%) calculated on the weight of the dried *R. typhi* cells. Lipid A was obtained from the LPS after hydrolysis with aqueous 1% (v/v) acetic acid at 100°C for 1 hr and keeping the hydrolyzate at -20°C overnight. The insoluble lipid A was separated from the hydrolysis mixture by centrifugation. The pellet was washed twice with deionized water followed by the centrifugation to remove residual polysaccharide, dispersed in deionized water, and lyophilized.

General and analytical methods. The isolated LPS was run on SDS-PAGE and stained with silver as described (Škultéty and Toman, 1992). The LPS was hydrolyzed with 2 mol/l trifluoroacetic acid at 120°C for 3 hrs and the neutral and amino sugars were analyzed as the corresponding alditol acetates by GC and GC-MS as reported (Škultéty *et al.*, 1998). After hydrolysis of LPS and lipid A in 2 mol/l hydrochloric acid in dry methanol for 2 and 16 hrs, the released fatty acids were analyzed directly and after trimethylsilylation by GC and GC-MS (Hussein *et al.*, 2001). Thin-layer chromatography of lipid A was accomplished on the pre-coated Silica Gel 60 plates (Merck) with isobutyric acid-1 mol/l ammonium hydroxide (5:3, v/v). Compounds were visualized by charring after spraying with 10% sulphuric acid in ethanol.

GC and GC-MS analyses. GC was performed with a Shimadzu Model 17A chromatograph equipped with the flame ionization detector using helium as the carrier gas. Alditol acetates of neutral sugars were separated on an SP-2330 column (30 m x 0.25 mm, Supelco) using a temperature program of 80°C for 2 mins, 30°C/min to 180°C, 4°C/min to 245°C, and 18 mins at 245°C. Alditol acetates of amino sugars were separated on an HP-5 column (25 m x 0.32 mm, Hewlett Packard) using a temperature program of 80°C for 1 min, 12°C/min to 180°C, hold 1 min at 180°C, 3°C/min to 210°C, and 15 mins at 210°C. Fatty acid methyl esters and their trimethylsilylated derivatives were separated on a DB-1 column (60 m x 0.25 mm, Fison, UK) using a temperature program of 80°C for 2 mins, 20°C/min to 160°C, 4°C/min to 236°C, 2°C/min to 300°C, and 5 mins at 300°C. The identity of each fatty acid was established by the comparison of its MS profile with that of the reference compound. GC-MS was performed on a Shimadzu model QP5000 instrument with helium as the carrier gas. Electron impact mass spectra were recorded at 70 eV and an ion-source temperature of 250°C. GC-MS was run with the columns and temperature programs already described for GC.

ESI-MS. ESI mass spectra were acquired with a Q-Tof Premier instrument (Waters). The lipid A samples were extracted with chloroform-methanol (1:1, v/v) at a concentration of the mixture 1 mg/ml. Samples were infused by a nanocapillary into ESI chamber at a flow rate of 1 μl/min. The nanospray pressure was 5 x 10^4 Pa and the cone gas was delivered at the rate of 20 l/hr. The source temperature was maintained at 30°C. Argon was used as the collision gas. MS/MS experiments were performed with the collision energies of 90–100 eV. Data were acquired from *m/z* 100 to 2200. The spectra were averaged and smoothed using a Savitzky-Golay smooting procedure (Micromass). Calculated monoisotopic masses were obtained from MolE web (Molecular Mass Calculator v2.0) http://www.sisweb.com/referenc/tools/exactmass.htm.

Results and Discussion

Isolation and characterization of LPS from R. typhi

LPS was isolated from the purified and enzyme-digested bacteria by a conventional hot phenol/water method. LPS was found in the phenol layer, and after subsequent dialysis and lyophilization, its yield was 2%. SDS-PAGE

of the LPS gave a „ladder-like" banding pattern typical for LPSs having a regular structure of the O-specific chain. The compositional analysis accomplished by GC and GC-MS revealed the presence of D-glucose (Glc), quinovosamine (QuiN, 2-amino-2,6-dideoxy-D-glucose), and D-glucosamine (GlcN) in a molar ratio 1.3:1.0:0.3, respectively. Colorimetric analyses indicated the presence of 3-deoxy-D-*manno*-2-oct-ulosonic acid and phosphate. Analyses of fatty acids revealed the presence of 3-hydroxytetradecanoic [C14:0(3-OH)], 3-hydroxy-hexadecanoic [C16:0(3-OH)], hexadecanoic (C16:0), and octadecanoic (C18:0) acids in a molar ratio 2.2:2.1:1.3:1.0, respectively.

Isolation of lipid A

Lipid A was released from the parent LPS upon treatment with a mild acid and separated from the hydrolysis mixture by centrifugation. Fatty acids released after methanolysis were analyzed directly and after trimethylsilylation by GC and GC-MS. Both their composition and molar ratio cor-responded to those given above. The chloroform-methanol extract of lipid A was directly analyzed by ESI-MS.

ESI-MS of lipid A

The ESI-MS spectrum of lipid A in the negative ion mode revealed the intense, singly charged ions at m/z 1420.5, 1392.3, 1194.3, and 1166.1 that represented monophosphor-ylated tetra- and triacylated molecular species of lipid A (Fig. 1, Table 1). An intense ion at m/z 1420.5 corresponded to two GlcN, one phosphate, one C14:0(3-OH), two C16:0(3-OH), and one C18:0 fatty acid residues. The signal at m/z 1392.3 corresponded to two GlcN, one phosphate, one C14:0(3-OH), two C16:0(3-OH), and one C16:0, i.e. a tetraacylated form of lipid A, too. We assume, however, that this signal should be attributed to a minor monophosphorylated tetraa-cylated molecular species of lipid A that differs from the major one at m/z 1420.5 by 28 mass units ($2\ CH_2$). Thus, we suggest that lipid A consisted of at least two species, a major one that contained C18:0 in its molecule and a minor one in which C18:0 was replaced by C16:0. A more detailed
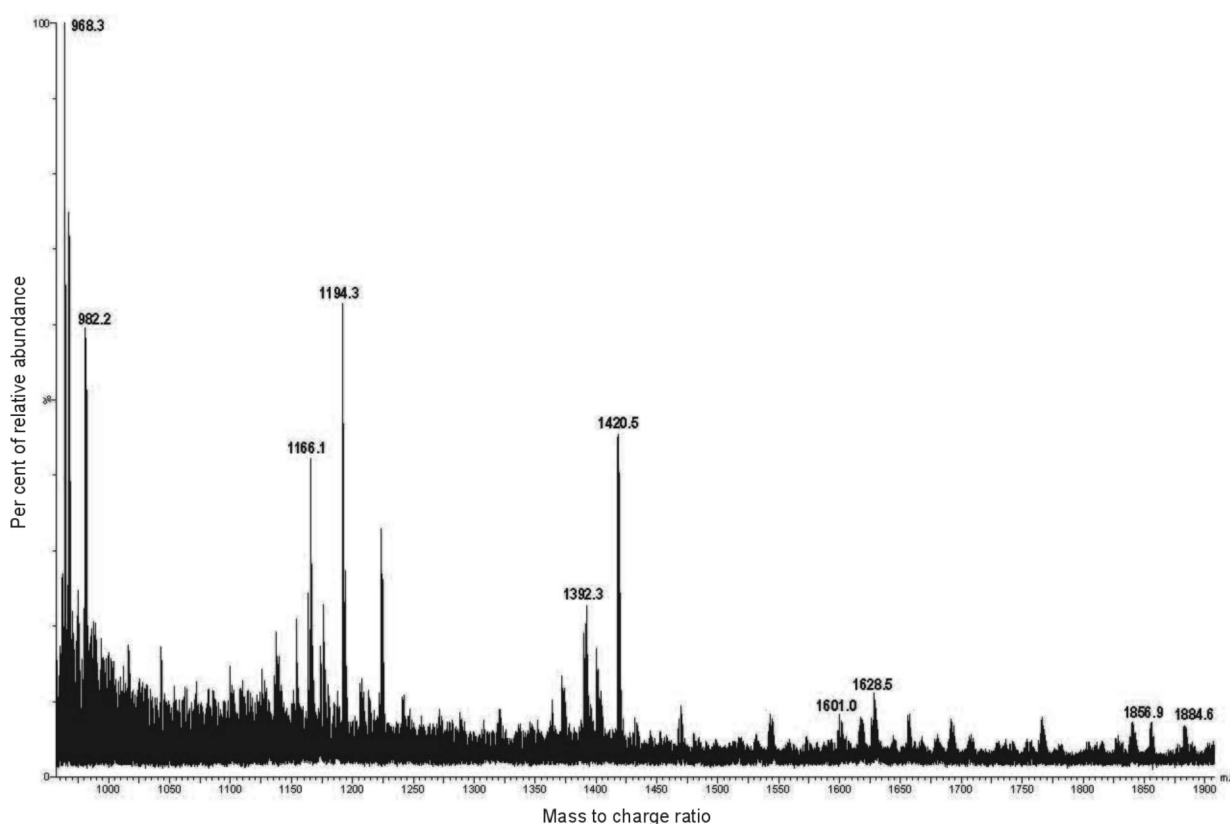
Fig. 1

ESI-MS spectrum (- ion mode) of lipid A of *R. typhi*

Axis x: mass to charge ratio; axis y: percentage of relative abundance.

confirmation of this assumption is given below. The intense peaks at *m/z* 1194.3 and 1166.1 represented the triacylated molecules in both lipid A species. The former ion should correspond with its mass to the major species consisting of two GlcN, one phosphate, two C16:0(3-OH) and one C18:0, and the latter to the minor lipid A species consisting of two GlcN, one phosphate, two C16:0(3-OH), and one C16:0.

In the lower molecular mass range of the spectrum, two intense peaks at *m/z* 982.2 and 968.3 were assigned to the doubly charged molecular species that represented the diphosphorylated hexaacylated lipid A forms. The former peak should belong to the major lipid A species containing two GlcN, two phosphates, two C14:0(3-OH), two C16:0(3-OH), one C16:0, and one C18:0. The latter peak should belong to the minor lipid A species with two GlcN, two phosphates, two C14:0(3-OH), two C16:0(3-OH), and two C16:0 in their molecules.

The low intensity ions at *m/z* 1628.5 and 1601.0 might represent the monophosphorylated pentaacylated forms of both major and minor lipid A species, respectively. Thus, the peak at *m/z* 1628.5 corresponded with its mass to two GlcN, one phosphate, two C14:0(3-OH), two C16:0(3-OH), and one C18:0, and the peak at *m/z* 1601.0 represented two

GlcN, one phosphate, two C14:0(3-OH), two C16:0(3-OH), and one C16:0.

There were also found two faint peaks at *m/z* 1884.6 and 1856.9 in the mass spectrum that could be attributed to the monophosphorylated hexaacylated forms of both major and minor lipid A species. The signal at *m/z* 1884.6 should correspond to two GlcN, one phosphate, two C14:0(3-OH), two C16:0(3-OH), one C16:0 and C18:0, and the peak at *m/z* 1856.9 represented two GlcN, one phosphate, two C14:0(3-OH), two C16:0(3-OH), and two C16:0. It is evident that the ESI-MS spectrum showed a pattern of molecular forms most probably due to the microheterogeneity of lipid A of *R. typhi* (Fig. 1). It cannot be excluded, however, that some of these forms could arise during the isolation of lipid A from the parent LPS or could be the products of the fatty acid eliminations during the ESI-MS measurements.

MS/MS analysis of the major, hexaacylated lipid A species at m/z 1884.6

In the MS/MS spectrum of the ion at *m/z* 1884.6, we observed besides the other fragment ions also those with
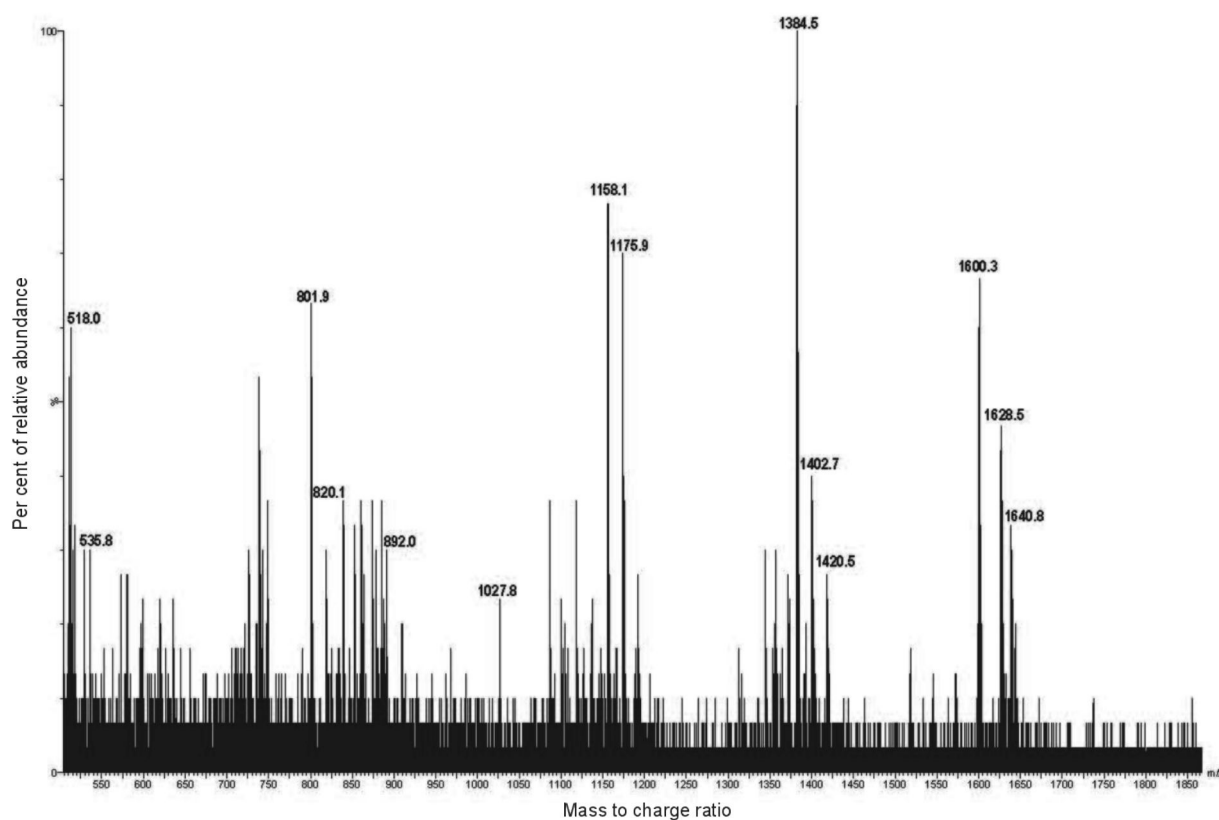
Fig. 2

ESI-MS/MS spectrum (- ion mode) of the ion at *m/z* 1884.6

Axis x: mass to charge ratio; axis y: percentage of relative abundance.

Table 1. Assignment of ions observed in ESI-MS and MS/MS spectra of lipid A species of *R. typhi*

Molecular mass		Proposed interpretation
Observed	Calculated	
MS		
1884.6	1885.4	$[M_1\text{-}H]^-$
1856.9	1857.4	$[M_1{}'\text{-}H]^-$
1628.5	1629.2	$[M_2\text{-}H]^-$ or $[M_1\text{-}H]^-$ – C16:0 – H_2O
1601.0	1601.2	$[M_2{}'\text{-}H]^-$ or $[M_1{}'\text{-}H]^-$ – C16:0 – H_2O
1420.5	1421.0	$[M_3\text{-}H]^-$ or $[M_1\text{-}H]^-$ – C14:0[3-O(C16:0)][a] or – C16:0 – H_2O – C14:1n3[a]
1392.3	1393.0	$[M_3{}'\text{-}H]^-$ or $[M_1{}'\text{-}H]^-$ – C14:0[3-O(C16:0)][a] or – C16:0 – H_2O – C14:1n3[a]
1194.3	1194.8	$[M_4\text{-}H]^-$
1166.1	1166.8	$[M_4{}'\text{-}H]^-$
982.2	982.7	$[M\text{ -2 }H]^{2-}$
968.3	968.7	$[M'\text{-2 }H]^{2-}$
MS/MS of m/z	**1884.6**	
1640.8	1641.2	$[M_1\text{-}H]^-$ – C14:0(3-OH) – H_2O
1628.5	1629.2	$[M_1\text{-}H]^-$ – C16:0 – H_2O
1600.3	1601.2	$[M_1\text{-}H]^-$ – C16:0 – H_2O
1420.5	1421.0	$[M_1\text{-}H]^-$ – C14:0[3-O(C16:0)][a] or – C16:0 – H_2O – C14:1n3[a]
1402.7	1403.0	$[M_1\text{-}H]^-$ – C14:0[3-O(C16:0)] – H_2O or – C16:0 – H_2O – C14:1n3 – H_2O or – C16:0 – H_2O – C14:0(3-OH)[a]
1384.5	1385.0	$[M_1\text{-}H]^-$ – C16:0 – H_2O – C14:0(3-OH) – H_2O or – C14:0(3-OH) – H_2O – C16:0 – H_2O
1175.9	1176.8	$[M_1\text{-}H]^-$ – C14:0[3-O(C16:0)][a] – C14:0(3-OH) – H_2O or – C14:0(3-OH) – H_2O – C14:0[3-O(C16:0)][a] or – C16:0 – H_2O – C14:0(3-OH) – H_2O – C14:1n3[a] or – C16:0 – H_2O – C14:1n3[a] – C14:0(3-OH) – H_2O or – C16:0 – H_2O – C14:0(3-OH)[a] – C14:1n3 – H_2O
1158.1	1158.8	$[M_1\text{-}H]^-$ – C16:0 – H_2O – C14:0(3-OH) – H_2O – C14:1n3 – H_2O or – C16:0 – H_2O – C14:1n3 – H_2O – C14:0(3-OH) – H_2O or – C14:0(3-OH) – H_2O – C14:0[3-O(C16:0)] – H_2O or – C14:0[3-O(C16:0)] – H_2O – C14:0(3-OH) – H_2O
1027.8	1028.7	$^{0,4}A$ – C16:0 – H_2O – C14:0(3-OH)[a]
892.0	892.5	$[M_1\text{-}H]^-$ – C14:0[3-O(C16:0)][a] – C14:0(3-OH) – H_2O – C18:0 – H_2O or – C14:0(3-OH) – H_2O – C14:0[3-O(C16:0)][a] – C18:0 – H_2O or – C16:0 – H_2O – C14:0(3-OH) – H_2O – C14:1n3[a] – C18:0 – H_2O or – C16:0 – H_2O – C14:1n3[a] – C14:0(3-OH) – H_2O – C18:0 – H_2O or – C16:0 – H_2O – C14:0(3-OH)[a] – C14:1n3 – H_2O – C18:0 – H_2O
820.1	820.5	$^{0,4}A$ – C14:0[3-O(C16:0)][a] or – C16:0 – H_2O – C14:1n3[a] or – C16:0 – H_2O – C14:0(3-OH)[a] –C14:1n3[a]
801.9	802.5	$^{0,4}A$ – C14:0[3-O(C16:0)] – H_2O or – C16:0 – H_2O – C14:0(3-OH)[a] – C14:1n3 – H_2O or – C16:0 – H_2O – C14:1n3 – H_2O
535.8	536.3	$^{0,4}A$ – C16:0 – H_2O – C14:0(3-OH)[a] – C14:1n3[a] – C18:0 – H_2O or – C14:0[3-O(C16:0)][a] – C18:0 – H_2O or – C16:0 – H_2O – C14:1n3[a] – C18:0 – H_2O
518.0	518.3	$^{0,4}A$ – C14:0[3-O(C16:0)] – H_2O – C18:0 – H_2O or – C16:0 – H_2O – C14:0(3-OH)[a] – C14:1n3 – H_2O – C18:0 – H_2O or – C16:0 – H_2O – C14:1n3 – H_2O – C18:0 – H_2O
MS/MS of m/z	**1420.5**	
1175.9	1176.8	$[M_3\text{-}H]^-$ – C14:0(3-OH) – H_2O
1136.4	1136.7	$[M_3\text{-}H]^-$ – C18:0 – H_2O
892.0	892.5	$[M_3\text{-}H]^-$ – C14:0(3-OH) – H_2O – C18:0 – H_2O or – C18:0 – H_2O – C14:0(3-OH) – H_2O
820.1	820.5	$^{0,4}A$
535.8	536.3	$^{0,4}A$ – C18:0 – H_2O
MS/MS of m/z	**1392.3**	
1148.3	1148.8	$[M_3{}'\text{-}H]^-$ – C14:0(3-OH) – H_2O
1136.0	1136.7	$[M_3{}'\text{-}H]^-$ – C16:0 – H_2O
1079.1	1079.4	$^{0,2}A$

Table 1. (continued)

Molecular mass		Proposed interpretation
Observed	Calculated	
892.0	892.5	$[M_3'-H]^- - C14:0(3\text{-}OH) - H_2O - C16:0 - H_2O$ or $- C16:0 - H_2O - C14:0(3\text{-}OH) - H_2O$
792.8	792.5	$^{0,4}A$
536.0	536.3	$^{0,4}A - C16:0 - H_2O$
MS/MS of *m/z*	**1194.3**	
910.2	910.6	$[M_4\text{-}H]^- - C18:0 - H_2O$
880.9	881.6	$^{0,2}A$
820.1	820.5	$^{0,4}A$
596.6	597.4	$^{0,2}A - C18:0 - H_2O$
535.8	536.3	$^{0,4}A - C18:0 - H_2O$
MS/MS s *m/z*	**1166.1**	
910.2	910.6	$[M_4'\text{-}H]^- - C16:0 - H_2O$
853.0	853.1	$^{0,2}A$
792.8	792.5	$^{0,4}A$
596.6	596.8	$^{0,2}A - C16:0 - H^2O$
536.0	536.3	$^{0,4}A - C16:0 - H_2O$

M and M´ correspond to molecular masses of diphosphorylated hexaacyl major and minor lipid A species, respectively. M_1–M_4 and M_1'–M_4' correspond to molecular masses of monophosphorylated hexa-, penta-, tetra-, and triacyl major and minor lipid A species, respectively. [a]Fatty acid eliminated as a ketene derivative. [b] $^{0,2}A$ and $^{0,4}A$ correspond to cross-ring fragments with cleavage in the sugar ring of GlcN I. Molecular masses were calculated as the monoisotopic masses from http://www.sisweb.com/referenc/tools/exactmass.htm.

a high intensity at *m/z* 1600.3, 1384.5, 1158.1, and 801.9 (Fig. 2, Table 1). The origin of the ion at *m/z* 1600.3 is not well understood at present. We assume that it might arise from the minor, monophosphorylated lipid A species after elimination of a free C16:0. The fragment ions at *m/z* 1384.5 and 1158.1 corresponded to the tetra- and triacylated lipid A forms, and the ion at *m/z* 801.9 represented the $^{0,4}A$ cleavage (Costello and Vath, 1990) of the ion at *m/z* 1402.7 (Schemes 1a, b and Table 1). Formation of these ions is explained in a more detail in the following text. The initial elimination of C14:0(3-OH) as a free fatty acid from the O-3 position of GlcN I of the monophosphorylated hexaacylated lipid A species gave rise to the ion at *m/z* 1640.8 (Scheme 1a, pathway a). Simultaneously, elimination of C16:0 as a free fatty acid from the hydroxyl group of C14:0(3-OH) linked to O-3´of GlcN II can take place giving rise to the ion at *m/z* 1628.5 (pathway b). The fragment ion at *m/z* 1420.5 corresponded to a loss of the acyl-oxyacyl group C14:0[3-O(C16:0)] from the O-3´position of GlcN II in the form of a ketene derivative (pathway c). This ion could also arise from the ion at *m/z* 1628.5 by elimination of C14:1n3 as a ketene derivative from the O-3´ position (pathway b₁). The ion at *m/z* 1402.7 indicated that C14:0[3-O(C16:0)] at the O-3´ position could be eliminated from the ion at *m/z* 1884.6 also as a free fatty acid (pathway d). The ion at *m/z* 1402.7 could be also formed by cleavage of C14:1n3 as a free

fatty acid from the O-3´ position of GlcN II (pathway b₂). Elimination of C14:0[3-O(C16:0)] as a ketene derivative or a free fatty acid indicated that this group was localized at O-3´of GlcN II. However, the ion at *m/z* 1402.7 could also arise in a different way, namely from the ion at *m/z* 1628.5 by an initial loss of C14:0(3-OH) as a ketene derivative from the O-3 position of GlcN I (Scheme 1b, pathway e).

The ion at *m/z* 1384.5 corresponded to a loss of C14:0(3-OH) as a free fatty acid from O-3 of the ion at *m/z* 1628.5 (Scheme 1a, pathway b). This ion could be also formed by elimination of C16:0 as a free fatty acid linked at O-3´ of the fragment ion at *m/z* 1640.8 (pathway a). The ion at *m/z* 1175.9 arose by elimination of C14:0(3-OH) as a free fatty acid from the ion at *m/z* 1420.5 (pathway c). An alternative pathway of the ion formation involves the loss of C14:1n3 as a ketene derivative from the ion at *m/z* 1384.5 (pathway f). Besides the given fragmentation pathways, the ion at *m/z* 1175.9 might arise by cleavage of C14:0[3-O(C16:0)] from the O-3´position of the ion at *m/z* 1640.8 in the form of a ketene derivative (pathway h). Elimination of C14:0(3-OH) as a free fatty acid at O-3 of the ion at *m/z* 1402.7 gave rise to the ion at *m/z* 1158.1 (pathway d). Another possible birth of this ion might proceed through elimination of C14:1n3 as a free fatty acid as it is given in the pathway g. Further, it could be formed from the ion at *m/z* 1640.8 after the loss of C14:0[3-O(C16:0)] from the O-3´position in the form of free fatty acid. (Scheme 1b,
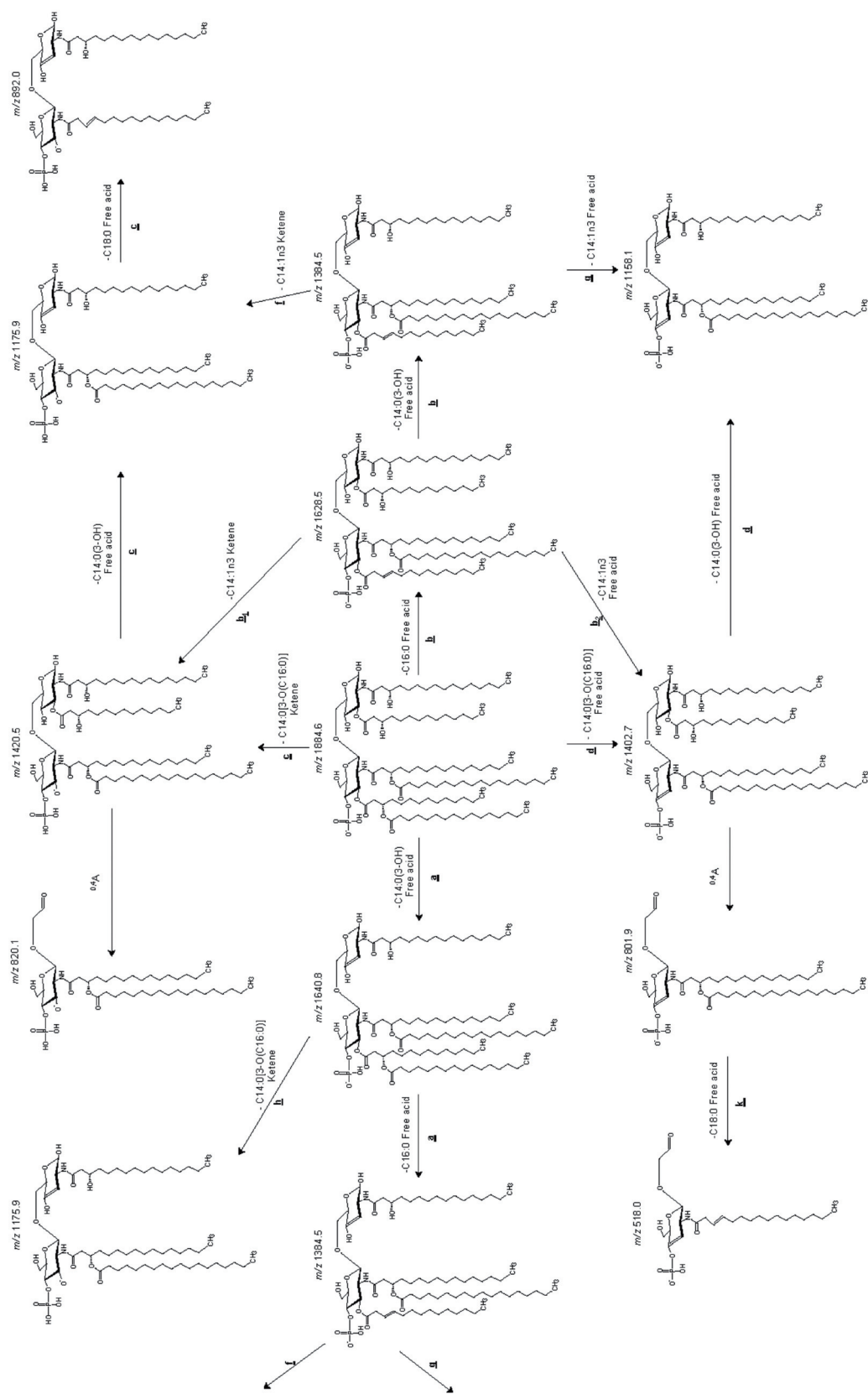
Scheme 1a

Fragmentation pathways of the lipid A precursor ion at *m/z* 1884.6

a, b, c, *etc.* denote the individual pathways.
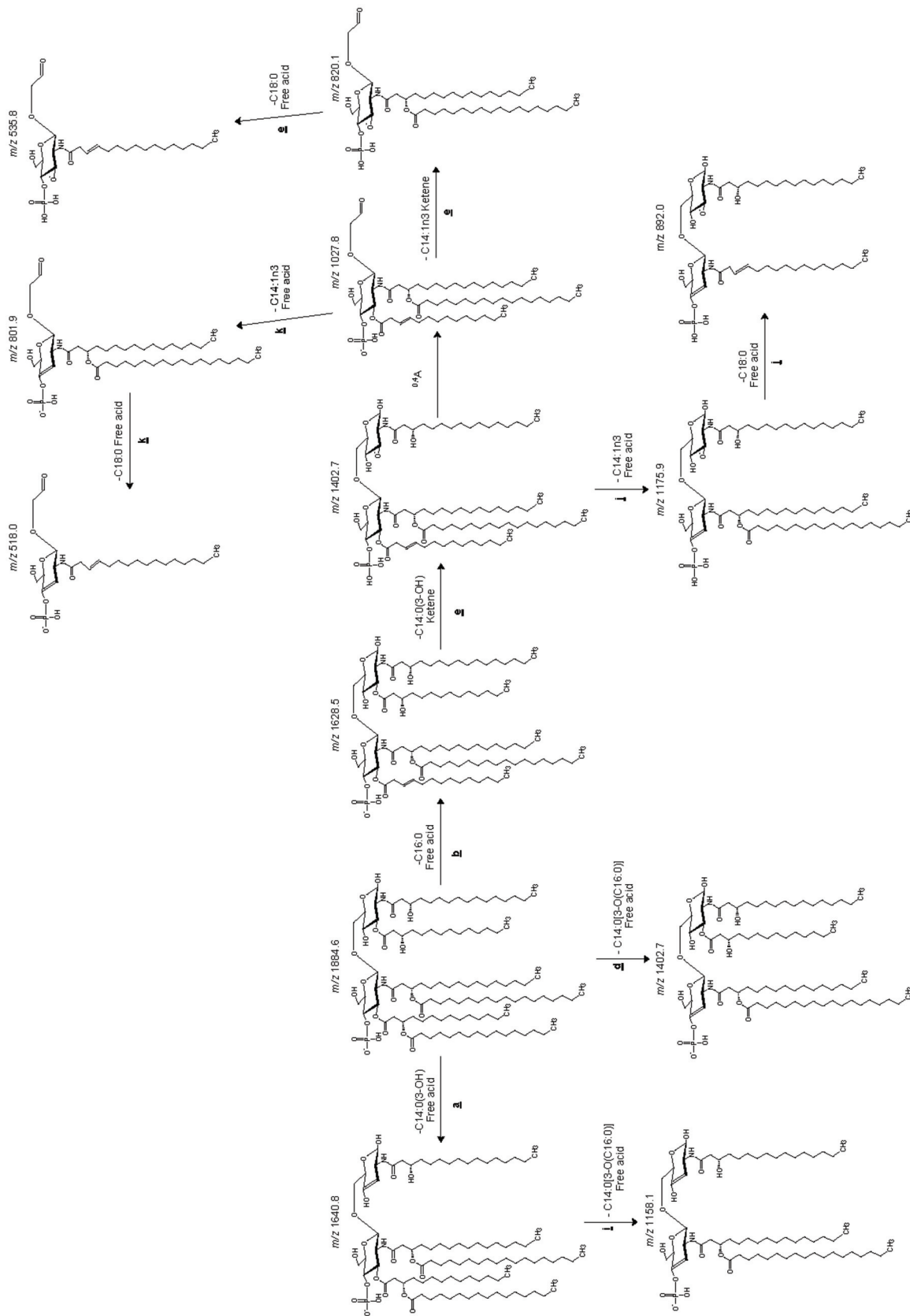
Scheme 1b

Fragmentation pathways of the lipid A precursor ion at *m/z* 1884.6

<u>a</u>, <u>b</u>, <u>c</u>, *etc.* denote the individual pathways.
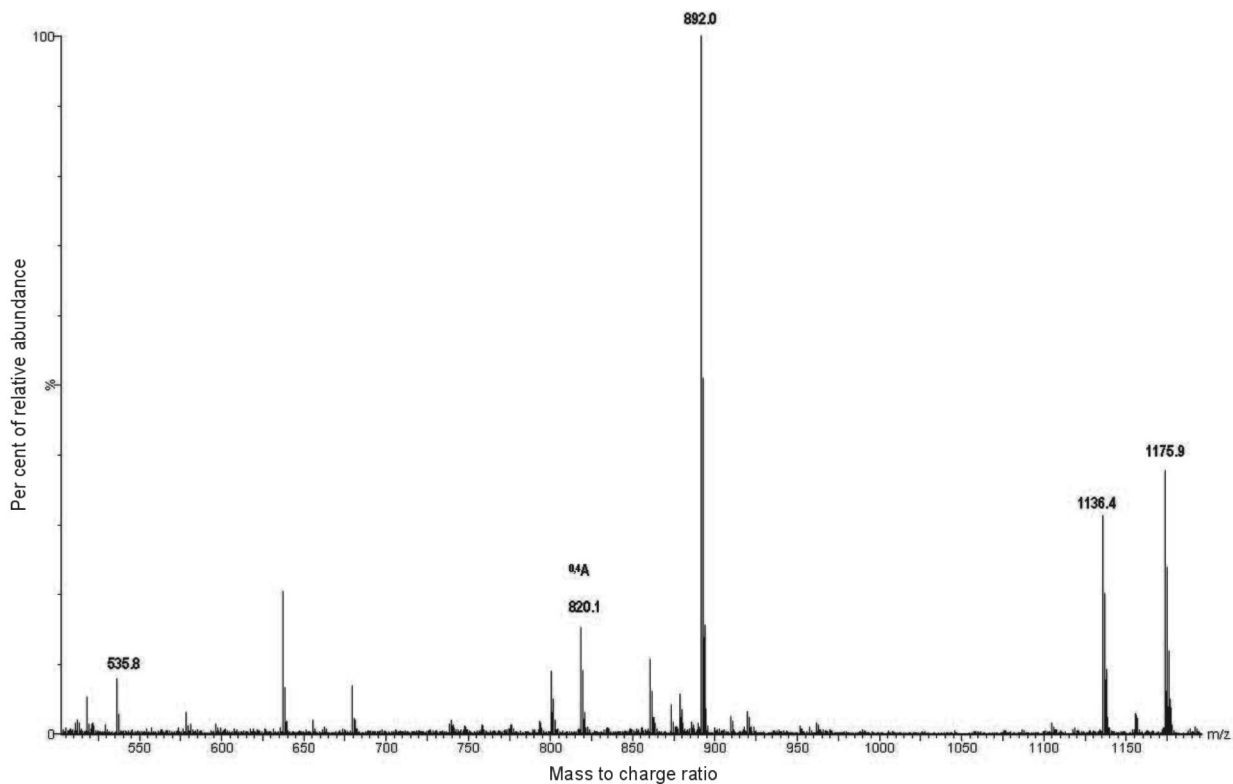
Fig. 3

ESI-MS/MS spectrum (- ion mode) of the ion at *m/z* 1420.5

Axis x: mass to charge ratio, axis y: percentage of relative abundance.
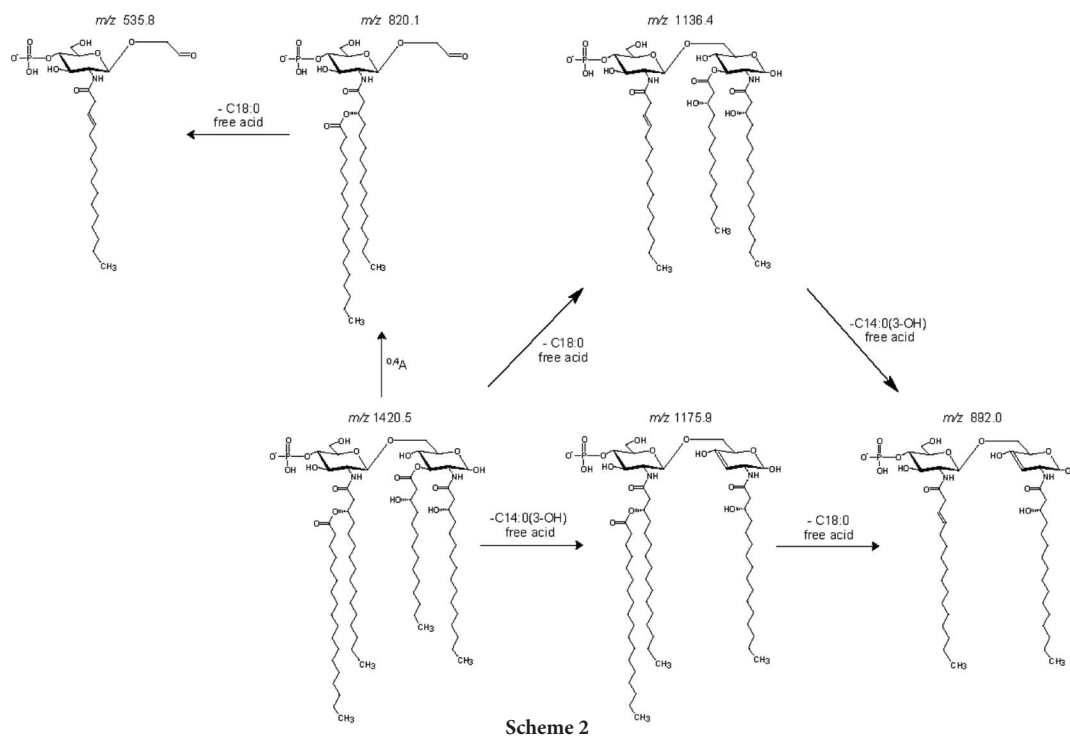
Scheme 2

Fragmentation pathways of the lipid A precursor ion at *m/z* 1420.5

Axis x: mass to charge ratio, axis y: percentage of relative abundance.
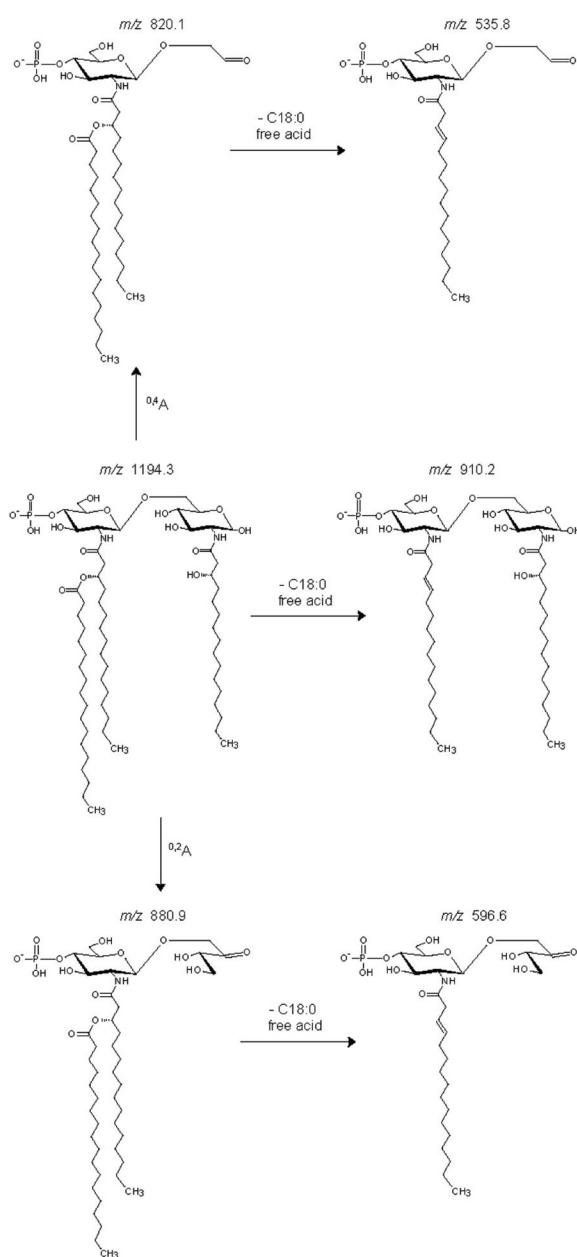
Scheme 3

Fragmentation pathways of the lipid A precursor ion at *m/z* 1194.3

pathway i̱). The loss of C18:0 as a free fatty acid from the ion at *m/z* 1175.9 gave rise to the ion at *m/z* 892.0 (Schemes 1a and 1b, pathways c̱, j̱, and Scheme 2). It is evident from the data presented that several ions with the identical *m/z* might arise by the alternative fragmentation pathways.

The fragment ion at *m/z* 820.1 could arise from the ion at *m/z* 1420.5 (Scheme 1a) by the ⁰,⁴A cleavage of GlcN I. The ion at *m/z* 801.9 arose from the ion at *m/z* 1402.7 in a similar way.

The ion at *m/z* 1027.8 could be formed by the ⁰,⁴A fragmentation of the isomeric ion with *m/z* 1402.7 (Scheme 1b). From this ion, the ion at *m/z* 820.1 was formed after the loss of C14:1n3 as a ketene derivative (pathway e̱). If C14:1n3 was eliminated as a free fatty acid, the ion at *m/z* 801.9 was formed (pathway ḵ). The subsequent elimination of C18:0 as a free fatty acid gives rise to the ion at *m/z* 518.0 (Schemes 1a and 1b, pathway ḵ). The ion at *m/z* 820.1 gave birth to the ion at *m/z* 535.8 after a loss of C18:0 as a free fatty acid (Scheme 1b, pathway e̱). Thus, the ⁰,⁴A fragment ions confirmed that C18:0 was secondary linked to amide-bound C16:0(3-OH) in GlcN II.

MS/MS analysis of the major, tetraacylated lipid A species at m/z 1420.5

The ion at *m/z* 1420.5 represented a monophosphorylated tetraacylated lipid A form with the composition given above. Its MS/MS gave a spectrum with three dominant fragment ions at *m/z* 1175.9, 1136.4 and 892.0 (Fig. 3, Table 1). The ion at *m/z* 1175.9 was generated due to the loss of C14:0(3-OH) as a free fatty acid from O-3 (Scheme 2). The ion at *m/z* 1136.4 was formed by elimination of C18:0 as a free fatty acid from the ion at *m/z* 1420.5. The most intense ion at *m/z* 892.0 might arise in two ways. The first involved a loss of C18:0 as a free fatty acid from the ion at *m/z* 1175.9, and the second, elimination of C14:0(3-OH) as a free fatty acid from the O-3 position of the ion at *m/z* 1136.4. The ion at *m/z* 820.1 arose through the ⁰,⁴A fragmentation of the ion at *m/z* 1420.5 and its further cleavage resulted in the ion with *m/z* 535.8.

MS/MS analysis of the major, triacylated lipid A species at m/z 1194.3

The ion at *m/z* 1194.3 represented a monophosphorylated triacylated lipid A form with the composition given above. Its MS/MS gave a spectrum with three dominant fragment ions at *m/z* 910.2, 880.9 and 820.1(Fig. 4, Table 1). The ion at *m/z* 910.2 arose through elimination of C18:0 as a free fatty acid and the ion at *m/z* 880.9 was formed by the ⁰,²A fragmentation (Costello and Vath, 1990) of GlcN I from the precursor ion at *m/z* 1194.3 (Scheme 3). From the ion at *m/z* 880.9, the loss of C18:0 as a free fatty acid gave rise to the ion at *m/z* 596.6. The ion at *m/z* 820.1 was formed by the ⁰,⁴A fragmentation of the ion at *m/z* 1194.3. The subsequent elimination of C18:0 as a free fatty acid gave the ion at *m/z* 535.8.

MS/MS analysis of the minor, tetraacylated lipid A species at m/z 1392.3

The ion at *m/z* 1392.3 represented the minor, monophosphorylated tetraacylated molecular species of lipid A (Fig. 1). Its composition is given above. MS/MS fragmenta-
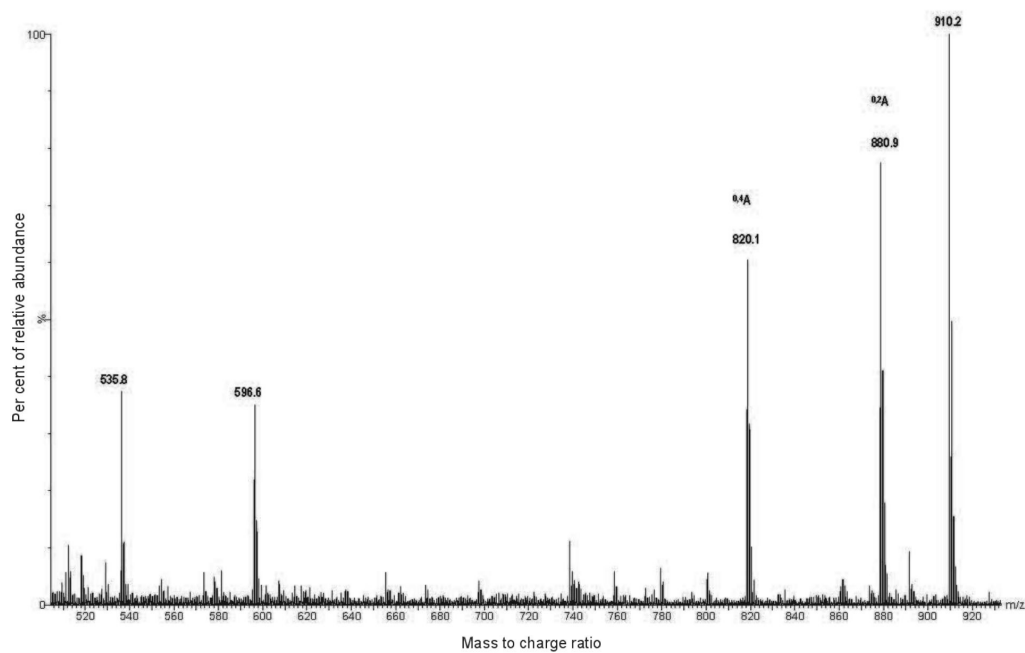
Fig. 4

ESI-MS/MS spectrum (- ion mode) of the ion at *m/z* 1194.3

Axis x: mass to charge ratio, axis y: percentage of relative abundance.
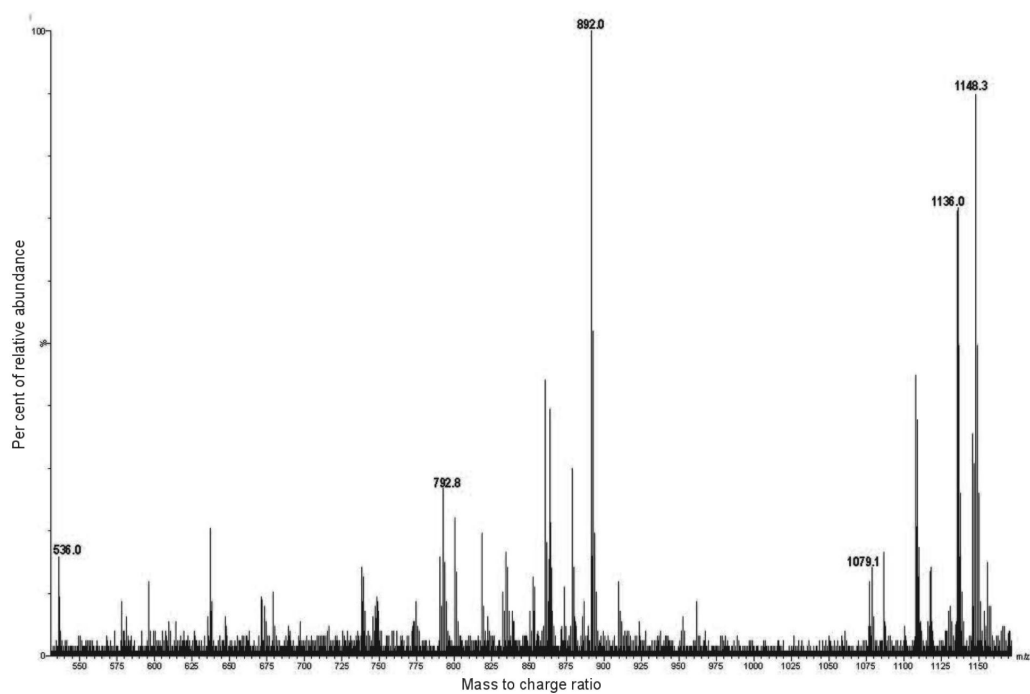
Fig. 5

ESI-MS/MS spectrum (- ion mode) of the ion at *m/z* 1392.3

Axis x: mass to charge ratio, axis y: percentage of relative abundance.
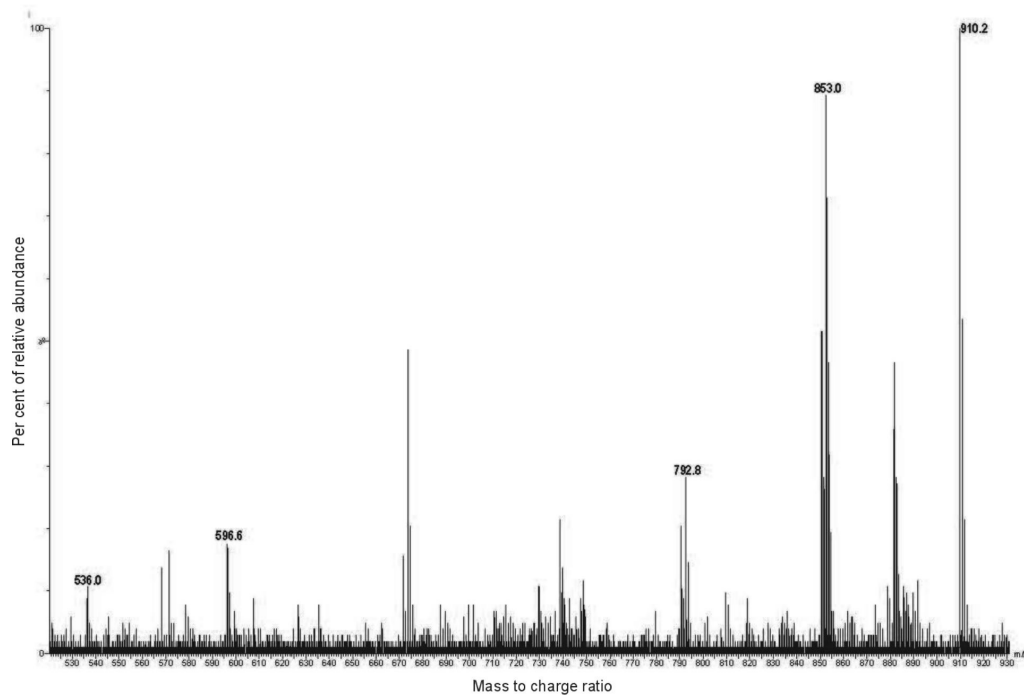
Fig. 6

ESI-MS/MS spectrum (- ion mode) of the ion at *m/z* 1166.1

Axis x: mass to charge ratio, axis y: percentage of relative abundance.
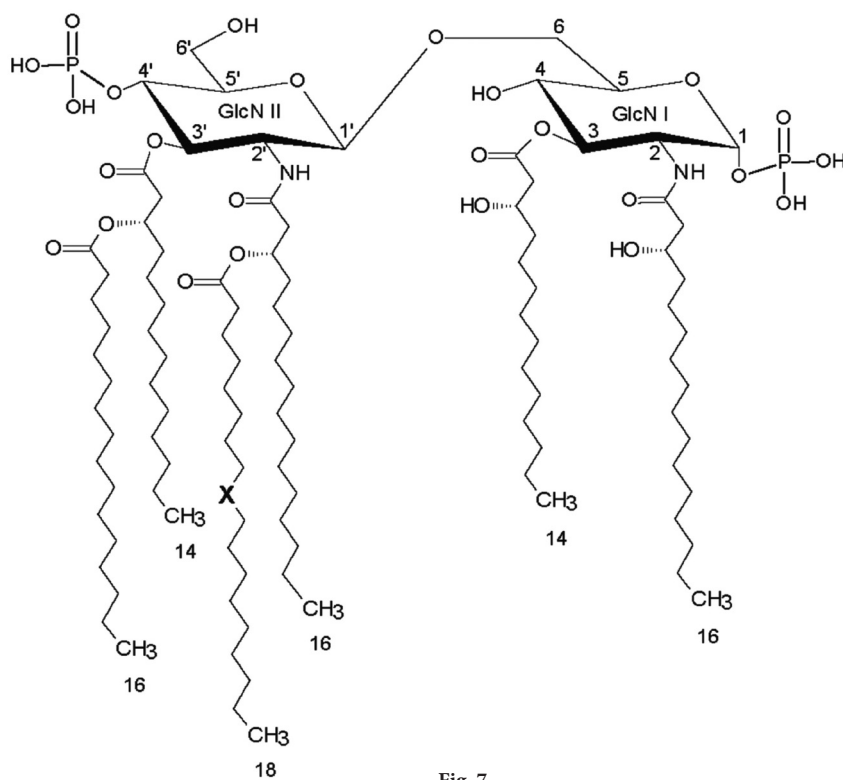
Fig. 7

Structural features of lipid A of *R. typhi*

X = C18:0 or C16:0 for the major or minor molecular species of lipid A, respectively.

tion gave the intense ions at *m/z* 1148.3, 1136.0 and 892.0 (Fig. 5, Table 1) following the pathways similar to those shown in Scheme 2. In this case, however, C16:0 was eliminated instead of C18:0 from the hydroxyl group of amide-linked C16:0(3-OH) in GlcN II. The ^{0,2}A and ^{0,4}A fragmentations of GlcN I resulted in the formation of ions at *m/z* 1079.1 and 792.8, respectively. From the latter ion, elimination of C16:0 as a free fatty acid gave rise to the ion at *m/z* 536.0.

MS/MS analysis of the minor, triacylated lipid A species at m/z 1166.1

The ion at *m/z* 1166.1 represented the minor, monophosphorylated triacylated molecular species of lipid A (Fig. 1). Its composition is given above. MS/MS fragmentation gave the ions at *m/z* 910.2, 853.0, 792.8, 596.6, and 536.0 (Fig. 6, Table 1) in the same manner as that shown for the ion at *m/z* 1194.3 (Scheme 3). In this case, however, C16:0 was eliminated instead of C18:0.

Conclusion

From our studies we concluded that the major *R. typhi* lipid A species represented the hexaacyl form (Fig. 7) resembling classical lipids A found in the family *Enterobacteriaceae*. It consisted of the β-(1→6)-linked GlcN disaccharide backbone carrying two phosphate groups. One of them was linked to the glycosidic hydroxyl group of GlcN I and the other one was ester-linked to the O-4′ position of GlcN II. The primary fatty acids consisted of two C14:0(3-OH) and two C16:0(3-OH). The former were ester- and the latter amide-linked to both GlcN. Two secondary fatty acids were represented by C18:0 and C16:0 that were ester-linked at the positions N-2′ and O-3′, respectively. Our MS analyses also revealed the presence of one minor molecular lipid A species in which ester-linked C18:0 was substituted by C16:0 at C16:0(3-OH) of GlcN II.

Our studies revealed a noticeable compositional and structural heterogeneity of lipid A of *R. typhi* with respect to the content of phosphate groups and the degree of acylation. The significance of the acyl pattern variation in the investigated lipid A is still unclear, but it may play a role in the biological activities (Alexander and Rietschel, 2001). Moreover, it is well known that enteric bacteria can synthetize different forms of lipid A in response to the host environment. On the other hand, we assumed that a part of the observed heterogeneity in the investigated lipid A could be generated by its incomplete biosynthesis in the living bacterium and by degradation processes during its isolation from the parent LPS. Thus, the presence of other lipid A isoforms in the *R. typhi* lipid A cannot be

excluded. In conclusion, the structural features of lipid A of *R. typhi* resemble classical forms of enterobacterial lipids A and this fact may indicate a high endotoxic potency of the whole bacterium (Zähringer *et al.*, 1999). However, more detailed structure/function relationship studies have to be performed in future to throw more light on this important problem.

References

Alexander C, Rietschel ET (2001): Bacterial lipopolysaccharides and innate immunity. J. Endotoxin Res. 7, 167–202.

Amano K, Williams JC, Dasch GA (1998): Structural properties of lipopolysaccharides from Rickettsia typhi and Rickettsia prowazekii and their chemical similarity to the lipopolysaccharide from Proteus vulgaris OX19 used in the Weil-Felix test. Infect. Immun. 66, 923–926.

Azad AF, Radulovic S, Higgins JA, Noden BH, Troyer JM (1997): Flea-borne rickettsioses: ecologic considerations. Emerg. Infect. Dis. 3, 319–327.doi:10.3201/eid0303.970308

Costello CE, Vath JE (1990): Tandem mass spectrometry of glycolipids. Methods Enzymol. 193, 738–768. doi:10.1016/0076-6879(90)93448-T

Fumarola D, Munno I, Monno R, Miragliotta G (1979): Lipopolysaccharides of Rickettsiaceae and the Limulus endotoxic assay. G. Bacteriol. Virol. Immunol. 72, 40–43.

Hussein A, Škultéty Ľ, Toman R (2001): Structural analyses of the lipopolysaccharides from Chlamydophila psittaci strain 6BC and Chlamydophila pneumoniae strain Kajaani 6. Carbohydr. Res. 336, 213–223. doi:10.1016/S0008-6215(01)00263-4

Raoult D, Roux V (1997): Rickettsioses as paradigms of new or emerging infectious diseases. Clin. Microbiol. Rev. 10, 694–719.

Shirai A, Dietel JW, Osterman JV (1975): Indirect hemagglutination test for human antibody to typhus and spotted fever group rickettsiae. J. Clin. Microbiol. 2, 430–437.

Schramek Š, Brezina R, Kazár J (1977): Some biological properties of an endotoxic lipopolysaccharide from the typhus group rickettsiae. Acta Virol. 21, 439–441.

Snyder JC (1965): Typhus fever Rickettsiae. In Horsfall J, Tamm H (Eds): Viral and Rickettsial Infections of Man. J.B. Lippincott Company, Philadelphia, Montreal, pp. 1059–1094.

Škultéty Ľ, Toman R (1992): Improved procedure for the drying and storage of polyacrylamide slab gels. J. Chromatogr. 582, 249–252. doi:10.1016/0378-4347(92)80328-N

Škultéty Ľ, Toman R, Pätoprstý V (1998): A comparative study of lipopolysaccharides from two Coxiella burnetii strains considered to be associated with acute and chronic Q

fever. Carbohydr. Polymers 35, 189–194. doi:10.1016/S0144-8617(97)00246-4

Whiteford SF, Taylor JP, Dumler JS (2001): Clinical, laboratory, and epidemiologic features of murine typhus in 97 Texas children. Arch. Pediatr. Adolesc. Med. 155, 396–400.

Zähringer U, Lindner B, Rietschel ET (1994): Molecular structure of lipid A, the endotoxic center of bacterial lipopolysac-

charides. Adv. Carbohydr. Chem. Biochem. 50, 211–276. doi:10.1016/S0065-2318(08)60152-3

Zähringer U, Lindner B, Rietschel ET (1999): Chemical structure of lipid A: recent advances in structural analysis of biologically active molecules. In Brade H, Opal SM, Vogel SN, Morrison DC (Eds): Endotoxin in Health and Disease. Marcel Dekker, Inc., New York, pp. 93–114.